7.1 Modulators

B. Kuhlow

7.1.1 Introduction

Modulation of light is used for a number of applications including the impression of information onto optical beams, Q-switching of lasers, for generation of giant optical pulses, and optical beam deflection.

Besides direct modulation by changing the laser current there are two main methods in modulation: internal and external modulation. The internal modulation method uses a change of the quality factor, Q, in a laser cavity by inserting a modulator. Due to the very sensitive lasing condition on losses in the cavity a highly efficient switching operation can be obtained. Therefore, this method is used for laser Q-switching and for active mode locking to generate ultra-short optical pulses. Internal modulators are very similar to external modulators that are widely used. Therefore, the latter ones will be treated next in more detail. However, an important requirement for intracavity modulators is the use of low loss optical materials mostly combined with the shortest possible optical length.

Light modulation is defined as a change of the amplitude or intensity, phase, polarization, or frequency of an incident light wave. It can be caused by changing the refractive index, absorption coefficient, or direction of transmitted light in the modulator medium. Various physical effects are known for interaction of light with external forces. An easy and simple way to deflect or switch a light beam is to use mechanical methods, e.g. moving mirrors or shutters, but their modulation frequencies are rather low. Higher frequencies are attainable with electrical or optical addressable effects. Among these absorption changes in semiconductors and dyes may be efficient and fast but usable laser wavelengths are very limited. Of major importance, however, is the method of refractive index change in dielectrics and semiconductors, which is efficiently used in many kinds of optical modulators including the important electro-optic and acousto-optic modulators. Especially the electro-optic effect allows for much higher modulation frequencies than all other methods.

A large variety of modulation devices have been investigated [72Den, 84Yar, 97Lee]. But, generally, there is no single "best" modulator. The choice of device is highly dependent on the specific application. The simplest type of modulator is the temporal-only or point modulator, where the modulation signal at the output is identical within any cross-section perpendicular to the propagation of light beam. A more general modulation device performing both spatial and temporal modulation is usually called a spatial light modulator. A survey of different modulator types is given in [97Lee].

In what follows only bulk electro-optic and acousto-optic light modulators and deflectors as well as a few examples of electro-optic Kerr cells using liquids will be treated which all are of major importance in laser applications.

7.1.2 Light propagation in crystals

The basic idea behind electro-optic and acousto-optic devices is to alter the optical properties of a material with an applied voltage in a controlled way. In certain types of crystals it is possible to effect a change in the index of refraction that is proportional to an electric field or acoustic strain field. These are referred to, respectively, as the electro-optic and photoelastic effects. They allow widely used means of controlling the intensity or phase of light when propagating through the crystal.

For any anisotropic (optically inactive) crystal class there are in general two orthogonal linearly polarized waves (i.e. direction of $\boldsymbol{D}$) with corresponding different phase velocities (i.e. index of refraction) for a given wave vector. The mutually orthogonal polarization directions and the indices of refraction of the two waves are found most easily in terms of the index ellipsoid (or indicatrix) that is a construct with geometric characteristics [84Yar].

The index ellipsoid assumes its simplest form in the principal coordinate system as

$$\frac{x^2}{n_x^2} + \frac{y^2}{n_y^2} + \frac{z^2}{n_z^2} = 1 \; . \tag{7.1.1}$$

Here n_x, n_y, n_z are the principal values of refraction along the principal crystal axes x, y, z, which are the directions in the crystal along which $\boldsymbol{D}$ and $\boldsymbol{E}$ are parallel.

Three types of optical crystals are possible:

1. biaxial crystals ($n_x \neq n_y \neq n_z$),
2. uniaxial crystals ($n_x = n_y = n_\mathrm{o}$; $n_z = n_\mathrm{e}$),
3. and isotropic crystals ($n_x = n_y = n_z = n_\mathrm{o}$).

They are established by the optical symmetry of a crystal and the corresponding dielectric tensor. The existence of an "ordinary" and an "extraordinary" ray with different indices of refraction is called birefringence. For a general direction of propagation, the section of the ellipsoid through the origin perpendicular to this direction is an ellipse where the major and minor axes represent the two orthogonal polarizations of $\boldsymbol{D}$ and the indices of refraction for this particular direction of propagation.

An electric field applied to certain crystals causes a slight change in the index of refraction, due to a redistribution of bond charges at the atomic level and possibly a slight deformation of the crystal lattice. A similar effect can be obtained by an acoustic strain field. In general, these alterations are not isotropic; that is, the changes vary with direction in the crystal. The net result is a change in the inverse dielectric constants (impermeability) tensor $1/n_{ij}^2$ of the index ellipsoid in its general form:

$$\Delta\left(\frac{1}{n^2}\right)_{ij} = r_{ijk}E_k + s_{ijkl}E_kE_l + p_{ijkl}S_{kl} \; , \quad i,j,k,l = 1,2,3 = x,y,z \; , \tag{7.1.2}$$

where E_x, E_y, E_z are the components of the applied electrical field vector in principal coordinates and S_{kl} are the second-order strain tensor elements defined by the symmetric part of the deformation gradient $S_{kl} = (\partial u_k/\partial x_l + \partial u_l/\partial x_k)/2$, where $u_{l,k}$ is the displacement. A summation over repeated indices is assumed. The linear (or Pockels) electro-optic effect is represented by the third-rank tensor r_{ijk}. The quadratic (or Kerr) electro-optic effect and the photoelastic effect are represented by fourth-rank tensors s_{ijkl} and p_{ijkl}, respectively. Because of permutation symmetries the linear electro-optic tensor r_{ijk} reduces to a 6×3 matrix and the fourth-rank tensors s_{ijkl} and p_{ijkl} reduce to a 6×6 matrix each. This leads to contracted notations r_{ik} and s_{ij}, p_{ij}, where $i,j = 1,\ldots,6$ and $k = 1,2,3$. The form of these tensors, but not the magnitude of tensor elements, can be derived from symmetry considerations, which dictate which of the coefficients are zero, as well as the relationships between the remaining coefficients [67Nye, 72Wem, 84Yar].

Crystals lacking a center of symmetry are non-centrosymmetric and exhibit a linear (Pockels) electro-optic effect. The induced changes in the impermeability tensor are linear in an applied electric field. On the other hand, all crystals exhibit a quadratic (Kerr) electro-optic effect as well as a photoelastic effect. Then, the changes in the impermeability tensor elements are quadratic in an applied electric field. When the linear effect is present, it generally dominates over all quadratic effects.

7.1.3 Linear electro-optic effect

The Pockels effect is named after the German physicist Friedrich Carl Alwin Pockels (1865–1913) who studied this phenomenon extensively in the year 1893. An electric field applied in a general direction to a non-centrosymmetric crystal produces a linear change in the constants $(1/n^2)_i$ due to the linear electro-optic effect according to

$$\Delta\left(\frac{1}{n^2}\right)_i = r_{ik}E_k\ , \quad i = 1,\ldots,6 \quad \text{and} \quad k = 1,2,3 = x,y,z\ , \tag{7.1.3}$$

where r_{ik} are the elements of the linear electro-optic tensor in contracted notation and E_x, E_y, E_z are the components of the applied electrical field in principal coordinates. A summation over repeated indices k is assumed. Using the rules of matrix multiplication, we have, for example $\Delta\left(\frac{1}{n^2}\right)_6 = r_{61}E_1 + r_{62}E_2 + r_{63}E_3$.

The magnitude of $\Delta(1/n^2)$ is typically in the order of less than 10^{-5}. Therefore, these changes are small perturbations. The index ellipsoid in the presence of an electric field can be written as [84Yar]:

$$\left(\frac{1}{n_x^2} + r_{1k}E_k\right)x^2 + \left(\frac{1}{n_y^2} + r_{2k}E_k\right)y^2 + \left(\frac{1}{n_z^2} + r_{3k}E_k\right)z^2 + 2yzr_{4k}E_k + 2zxr_{5k}E_k + 2xyr_{6k}E_k = 1\ . \tag{7.1.4}$$

The presence of cross terms indicates that the ellipsoid is rotated and the lengths of the principal dielectric axes are changed. A new set of principal axes x', y', and z' can always be found by a coordinate rotation where the perturbed ellipsoid will be represented again in the standard form, see (7.1.1),

$$\frac{x'^2}{n_{x'}^2} + \frac{y'^2}{n_{y'}^2} + \frac{z'^2}{n_{z'}^2} = 1 \tag{7.1.5}$$

with eigenvalues $1/n_{x'}^2$, $1/n_{y'}^2$, $1/n_{z'}^2$ depending on the strength and direction of the applied field and of course on the given matrix elements r_{ij} for the used crystal class. Extensive tables of linear electro-optic coefficients are listed in [79Coo].

7.1.3.1 Modulator devices

An electro-optic modulator is a device with operation based on an electrically induced change in index of refraction or change in natural birefringence. Two types of modulators can be classified: *longitudinal* and *transversal* ones.

In the *longitudinal* configuration the voltage is applied parallel to the direction of light propagation in the device. The electrodes must be transparent for the light or a small aperture at the

center at each end of the crystal has to be introduced. The applied electric field inside the crystal is $E = V/L$, where L is the length of the crystal. The induced phase shift is proportional to the voltage V but not to physical dimensions of the device.

In *transverse* configuration the voltage is applied perpendicular to the direction of light propagation. The electrodes do not obstruct the light as it passes through the crystal. The applied electric field is $E = V/d$, where d is the lateral separation of the electrodes. Thus, the voltage necessary to achieve a desired degree of modulation can be largely reduced by reduction of d. However, the transverse dimension d is limited by the increase of capacitance, which affects the modulation bandwidth or speed of the device.

Different kinds of modulation can be obtained using an electro-optic bulk modulator in combination with polarizers and passive birefringence elements [84Yar, 95Mal]. Usually it is desirable to modulate only one optical parameter at a time; simultaneous changes in the other parameters must then be avoided. First, it is assumed that the modulation field is uniform throughout the length of the crystal and the modulation frequency is very low ($\omega_m \ll 2\pi c/nL$).

Examples of modulator devices using the linear electro-optic effect in KDP, ADP, $LiNbO_3$, $LiTaO_3$, GaSe, and the quadratic electro-optic effect in $BaTiO_3$ are given in [84Yar, 89Gha]. Pockels cells typically can be operated at fairly low voltages (roughly 5 to 10 times less than an equivalent Kerr cell) and the response time is shorter than for Kerr cells. The response time of KDP is less than 10 ps, and such a modulator can work up to about 25 GHz. In $LiNbO_3$ electro-optic modulation up to 50 GHz has been demonstrated [92Dol]. High-speed modulators above 40 GHz for telecommunication applications in combination with semiconductor lasers today are mostly based on electro-absorption effect in some special semiconductor materials [02Tak]. The following presentation corresponds widely to examples given in [84Yar, 95Mal].

7.1.3.1.1 Phase modulation

A light wave can be phase-modulated, without change in polarization or intensity, using a suitable cut of an electro-optic crystal. One of two possibilities is required for a crystal and its orientation:

1. A crystal having principal axes that will not rotate with applied voltage, but change uniformly. An example is $LiNbO_3$ with applied field along its optical z-axis. This solution is suitable for randomly polarized laser beams.
2. A crystal having a characteristic plane perpendicular to the direction of propagation where the plane rotates under the influence of an applied field. Then the input wave must be polarized along one of the new principal axes x' or y' and will not alter this polarization during modulation. An example is KDP with electric field applied along its optical z-axis. Such a configuration is shown in Fig. 7.1.1.

According to Fig. 7.1.1 with a polarizer along x' the optical wave at the output of the crystal exhibits a phase shift

$$\Delta\Phi = \frac{2\pi}{\lambda} \cdot \Delta n_{x'} \cdot L \; . \tag{7.1.6}$$

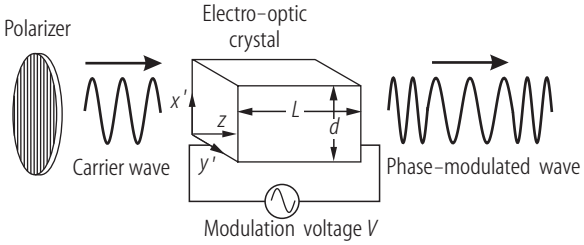

Fig. 7.1.1. Longitudinal phase modulator.

The electrically induced change in refractive index is $\Delta n_{x'} \approx -\frac{1}{2} n_{x'}^3 r E$, where r is the corresponding electro-optic coefficient.

For a *longitudinal* modulator with applied electrical field $E = V/L$ the induced phase shift is (apart of sign)

$$\Delta\Phi = \frac{\pi}{\lambda} \cdot n_{x'}^3 r V \,, \tag{7.1.7a}$$

which is independent of L and linearly proportional to V.

For a *transverse* modulator with applied electric field $E = V/d$ the induced phase shift is

$$\Delta\Phi = \frac{\pi}{\lambda} \cdot n_{x'}^3 r V \cdot \frac{L}{d} \,, \tag{7.1.7b}$$

which is a function of the aspect ratio L/d.

The half-wave voltage producing $\Delta\Phi = \pi$ for a longitudinal modulator is

$$V_\pi = \frac{\lambda}{n_{x'}^3 r} \tag{7.1.8a}$$

and for a transverse modulator

$$V_\pi = \frac{\lambda}{n_{x'}^3 r} \cdot \frac{d}{L} \,. \tag{7.1.8b}$$

If the applied modulation voltage and corresponding electric field is sinusoidal in time the phase at the output changes accordingly, as

$$\Phi = \frac{2\pi}{\lambda} \left(n_{x'} - \frac{1}{2} n_{x'}^3 r E_\mathrm{m} \cdot \sin\omega_\mathrm{m} t \right) \cdot L = \frac{2\pi}{\lambda} \cdot n_{x'} L - \delta \cdot \sin\omega_\mathrm{m} t \,. \tag{7.1.9}$$

Thus, the optical field is phase-modulated with phase-modulation index

$$\delta = \frac{\pi}{\lambda} \cdot n_{x'}^3 r E_\mathrm{m} L = \pi \cdot \frac{V_\mathrm{m}}{V_\pi} \,. \tag{7.1.10}$$

Neglecting a constant phase term, the output wave can be developed into a Bessel function series $E_0(t) = E_i \sum_n J_n(\delta) \cos(\omega + n\omega_\mathrm{m})t$ which consists of components at frequency ω and higher harmonic frequencies $(\omega + n\omega_\mathrm{m})$, $n = \pm 1, \pm 2, \ldots$ The distribution of energy into the sidebands is a function of modulation index δ.

7.1.3.1.2 Polarization modulation (dynamic retardation)

Polarization modulation involves the coherent addition of two orthogonal waves, resulting in a change of the input polarization state at the output. A suitable configuration is shown in Fig. 7.1.2. The crystal and applied voltage are configured to produce dynamically fast and slow axes in the crystal cross-section. The polarizer is positioned such that the input light is decomposed equally into the two orthogonal linear eigenpolarizations along these axes.

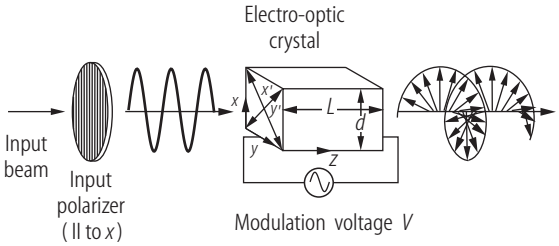

Fig. 7.1.2. Longitudinal polarization modulator with input polarizer oriented along the x principal axis at 45° with respect to the perturbed axes x' and y'.

If the light propagating along the z principal axis is polarized along the x- (or y-) axis the corresponding refractive indices of the fast and slow axes x' and y', respectively, are

$$n_{x'} \approx n_x - \frac{1}{2} n_x^3 r_x E \quad \text{and} \quad n_{y'} \approx n_y + \frac{1}{2} n_y^3 r_y E \,,$$

where n_x and n_y are the unperturbed indices of refraction and r_x, r_y are the corresponding electro-optic coefficients for the used material and orientation of the applied field. The phase difference or retardation is

$$\Gamma = \frac{2\pi}{\lambda} \cdot (n_{y'} - n_{x'}) \cdot L = \frac{2\pi}{\lambda} \cdot (n_y - n_x) \cdot L + \frac{\pi}{\lambda} \cdot \left(n_y^3 r_y + n_x^3 r_x\right) \cdot EL = \Gamma_0 + \Gamma_\mathrm{i} \,. \tag{7.1.11}$$

Γ_0 is the natural retardation without applied field and Γ_i is the field-induced part of the retardation. In general, the output wave is elliptically polarized. Special points are $\Gamma = \pi/2$, where the electrical field vector is circularly polarized, and $\Gamma = \pi$, where the wave is again linearly polarized, but rotated by 90° to its input direction of polarization. The half-wave voltage in this more general case of a longitudinal modulator is $V_\pi = \lambda/(n_y^3 r_y + n_x^3 r_x)$, which is proportional to the wavelength λ and inversely proportional to the relevant electro-optic coefficients. To cancel out an occurring natural birefringence, the phase retardation Γ_0 can be made a multiple of 2π by slightly polishing the crystal to adjust its length, or by introducing a variable compensator, or more practical by applying a bias voltage.

7.1.3.1.3 Amplitude modulation

The intensity of a light wave can be modulated in several ways. Some possibilities are:

1. including a dynamic retarder configuration with either crossed or parallel polarizer at the output, or
2. using a phase modulator configuration in one branch of a Mach–Zehnder interferometer, or
3. choosing a dynamic retarder with push–pull electrodes.

An intensity modulator constructed using a dynamic retarder with crossed polarizers, as shown in Fig. 7.1.3, yields for the transmission $T = I_\mathrm{o}/I_\mathrm{i}$, the ratio of output to input intensity, the relation

$$T(V) = \sin^2\left(\frac{\Gamma}{2}\right) = \frac{1}{2} \cdot [1 - \cos\Gamma] = \frac{1}{2} \cdot \left[1 - \cos\left(\Gamma_0 + \frac{\pi V}{V_\pi}\right)\right] \,. \tag{7.1.12}$$

For linear modulation around the 50% transmission point a fixed bias of $\Gamma_0 = \pi/2$ must be introduced, either by placing an additional phase retarder, a quarter-wave plate at the crystal output, or by applying a bias voltage of $V_\pi/2$. In case of natural birefringence the values have to be changed accordingly.

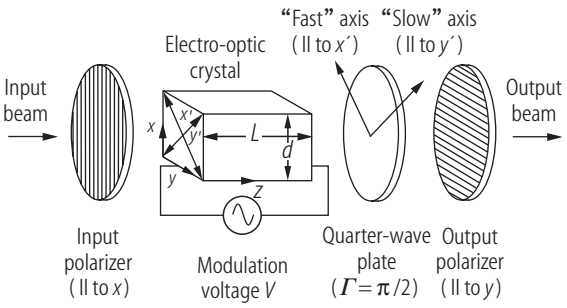

Fig. 7.1.3. Longitudinal intensity modulator using crossed polarizers and a quarter-wave plate as a bias to produce linear modulation.

For sinusoidal modulation of V the retardation at the output including bias is $\Gamma = \pi/2 + \Gamma_\mathrm{m} \sin \omega_\mathrm{m} t$, where the *amplitude modulation index* is

$$\Gamma_\mathrm{m} = \pi \cdot \frac{V_\mathrm{m}}{V_\pi} \,. \tag{7.1.13}$$

The transmission in case of $V_\mathrm{m} \ll 1$ becomes $T(V) = \frac{1}{2}[1+\Gamma_\mathrm{m} \sin \omega_\mathrm{m} t]$, which is linear proportional to the modulation voltage. If the signal is large, then the output intensity becomes distorted, and again higher-order odd harmonics appear.

7.1.3.1.4 Design considerations

Modulators operating in transverse configuration have a half-wave voltage typically in the order of tens of volts compared to about 10,000 V for longitudinal devices [89Gha]. For phase modulation, a crystal orientation is required that would give the maximum change in index of refraction, whereas for amplitude modulation a maximum birefringence must be produced.

For $L \ll 2\pi c/\omega_\mathrm{m} n$ the transit time $\tau = nL/c$ of light in the crystal is of no relevance for the modulation frequency and the electro-optic crystal can be modeled as a lumped capacitor. As the modulation frequency increases beyond such limit the optical phase no longer follows adiabatically the time-varying refractive index. The result is a reduction in the modulation index parameters, δ for phase modulation and Γ_m for amplitude modulation, by a factor

$$\sigma = \frac{\sin\left(\frac{1}{2}\omega_\mathrm{m}\tau\right)}{\left(\frac{1}{2}\omega_\mathrm{m}\tau\right)} = \mathrm{sinc}\left(\frac{1}{2}\omega_\mathrm{m}\tau\right) \,. \tag{7.1.14}$$

If $\tau = 2\pi/\omega_\mathrm{m}$ then the transit time of light is equal to the modulation period and the net retardation is reduced to zero. If, somewhat arbitrarily, one takes the highest useful modulation frequency from $\tau = \pi/\omega_\mathrm{m}$ it follows $(\nu_\mathrm{m})_\mathrm{max} = c/(2Ln)$. E.g. using a KDP crystal ($n = 1.5$) with a length of $L = 2$ cm, it yields $(\nu_\mathrm{m})_\mathrm{max} = 5$ GHz.

7.1.3.2 Traveling-wave modulator

Applying the modulation voltage as a traveling wave, propagating collinearly with the optical wave, can largely extend the limitation of the transit time on the bandwidth of a modulator. Figure 7.1.4 illustrates a transverse traveling-wave modulator. (The modulation field direction is along the x-axis, whereas both light and traveling wave propagate along z.) The electrode is designed to be part of the driving transmission line in order to eliminate electrode charging time effects on the bandwidth. Therefore, the transit time problem is addressed by adjusting the phase velocity of the modulation signal to be equal to the phase velocity of the optical signal [84Yar, 89Gha, 90Alf].

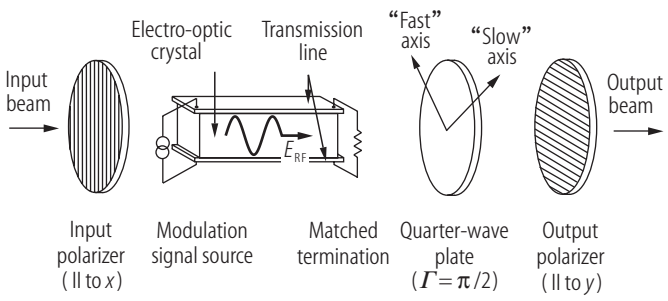

Fig. 7.1.4. Transverse traveling-wave electro-optic modulator.

A mismatch in the phase velocities of the modulating signal and optical wave will produce a reduction in the modulation index δ or Γ_m by a factor

$$\sigma_\mathrm{tw} = \mathrm{sinc}\,(qL) \ , \tag{7.1.15}$$

where

$$q = \frac{\omega_\mathrm{m}}{2c} \cdot (n_\mathrm{m} - n) = \frac{\omega_\mathrm{m}}{2} \cdot \left(\frac{1}{v_\mathrm{m}} - \frac{1}{v_0}\right) \ .$$

v_m and $n_\mathrm{m} = \sqrt{\varepsilon}$ are the phase velocity and index of refraction of the modulating signal, v_0 and n are the according terms for the light beam, respectively. In the case of amplitude modulation this equation holds only if there is no natural birefringence in the cross section of the crystal.

Whereas for low frequencies the modulation indices δ and Γ_m are linearly proportional to the crystal length L these become a sinusoidal function of L at higher frequencies. For a given mismatch q the maximum modulation index can be achieved for crystal lengths $L = \pi/2q$, $3\pi/2q$, etc. The always occurring mismatch between n_m and n produces a walk-off between the optical wave and the modulation wave. The maximum useful modulation frequency is taken to be $(\nu_\mathrm{m})_\mathrm{max} = c/[2L(n_\mathrm{m} - n)]$, showing an increase in the modulation frequency limit or useful crystal length by a factor of $\left(1 - \frac{n_\mathrm{m}}{n}\right)^{-1}$ for a traveling-wave modulator.

7.1.3.3 Examples

7.1.3.3.1 Crystal classes

7.1.3.3.1.1 Crystal class $\bar{4}$2m

Widely used modulator crystals such as KH_2PO_4 (KDP), KD_2PO_4 (KD*P), $(NH_4)H_2PO_4$ (ADP), $(NH_4)D_2PO_4$ (AD*P) belong to this crystal class.

These crystals are naturally uniaxial with optical axis along z. The three non-vanishing electro-optic tensor elements are $r_{41} = r_{52}$, r_{63}.

Applying a field along the z-axis gives from (7.1.4)

$$\frac{\left(x^2 + y^2\right)}{n_\mathrm{o}^2} + \frac{z^2}{n_\mathrm{e}^2} + 2r_{63}E_z \cdot xy = 1 \ ,$$

where n_o and n_e are the ordinary and extraordinary refractive indices, respectively. The new index ellipsoid resulting from rotation of the principal plane (x, y) by 45° is

$$\left(\frac{1}{n_\mathrm{o}^2} + r_{63}E_z\right) \cdot x'^2 + \left(\frac{1}{n_\mathrm{o}^2} - r_{63}E_z\right) \cdot y'^2 + \frac{z^2}{n_\mathrm{e}^2} = 1 \ .$$

The lengths of the major axes of this ellipsoid depend on the applied field. Assuming $r_{63}E_z \ll n_\mathrm{o}^{-2}$ gives the refractive indices of the two linearly polarized eigenmodes as $n_{x'} = n_\mathrm{o} - \frac{1}{2}n_\mathrm{o}^3 r_{63}E_z$ and $n_{y'} = n_\mathrm{o} + \frac{1}{2}n_\mathrm{o}^3 r_{63}E_z$. The birefringence of this plate is $n_{y'} - n_{x'} = n_\mathrm{o}^3 r_{63}E_z$ giving a phase retardation of $\Gamma = \frac{2\pi}{\lambda} \cdot n_\mathrm{o}^3 r_{63}V$ and a half-wave voltage of $V_\pi = \lambda/(2n_\mathrm{o}^3 r_{63})$. E.g. the half-wave voltage for a z-cut KDP plate at $\lambda = 633$ nm is 9.3 kV.

7.1.3.3.1.2 Crystal class 3m

The uniaxial crystals $LiNbO_3$ or $LiTaO_3$ belong to this crystal class. The non-vanishing electro-optic tensor elements are $r_{51} = r_{42}$, $r_{22} = -r_{12} = -r_{61}$, $r_{13} = r_{23}$, r_{33}.

z-cut: Applying a field along the optical z-axis of the crystal gives from (7.1.4)

$$\left(\frac{1}{n_o^2} + r_{13}E_z\right) \cdot x^2 + \left(\frac{1}{n_o^2} + r_{13}E_z\right) \cdot y^2 + \left(\frac{1}{n_e^2} + r_{33}E_z\right) \cdot z^2 = 1 \ .$$

The principal axes of the new index ellipsoid remain unchanged and the lengths of the new semi-axes are $n_x = n_o - \frac{1}{2}n_o^3 r_{13}E_z$, $n_y = n_o - \frac{1}{2}n_o^3 r_{13}E_z$, and $n_z = n_e - \frac{1}{2}n_e^3 r_{33}E_z$.

Under the influence of an applied electric field parallel to the z-axis (c-axis), the crystal remains uniaxially anisotropic. Light propagating along z will experience the same phase change regardless of its polarization state. Thus, an unpolarized laser can be modulated with such a device. In a longitudinal configuration the voltage-driven phase change is $\Delta\Phi = \frac{\pi}{\lambda} \cdot n_o^3 r_{13} V$ and the half-wave voltage for phase modulation is $V_\pi = \lambda/(n_o^3 r_{13})$. E.g. for $LiNbO_3$ at $\lambda = 633$ nm it results in $V_\pi = 5.5$ kV. Since no phase retardation between any two orthogonal polarized waves is introduced, no amplitude modulation can be achieved. Other z-cut uniaxial electro-optic crystals behave similar, except crystals with $\bar{4}2m$ or $\bar{4}$ symmetry, which become biaxial under the influence of an electric field.

x-cut: However, if the field is oriented along the z-axis and a light beam is propagating along the x-axis (or equivalently along the y-axis), a birefringence of $n_z - n_y = (n_e - n_o) - \frac{1}{2}(n_e^3 r_{33} - n_o^3 r_{13})\, E_z$ occurs. This can be used for a transverse modulator.

The phase retardation for light passing through the crystal is thus

$$\Gamma = \frac{2\pi}{\lambda} \cdot (n_e - n_o)L - \frac{\pi}{\lambda} \cdot (n_e^3 r_{33} - n_o^3 r_{13})V \cdot \frac{L}{d} \ .$$

For light linearly polarized along z direction the electrically induced phase change is $\Delta\Phi = \frac{\pi}{\lambda} \cdot n_e^3 r_{33} V \cdot \frac{L}{d}$. Because of the natural birefringence, an amplitude modulator using these crystals requires a phase compensator. The half-wave voltage in case of arbitrary polarization is

$$V_\pi = \frac{d}{L} \cdot \frac{\lambda}{(n_e^3 r_{33} - n_o^3 r_{13})} \ .$$

Thus, the half-wave voltage in a transverse modulator can be largely reduced by reduction of d. It typically lies in the range of 100 V (see Table 7.1.2). Transverse modulators using $LiNbO_3$ or $LiTaO_3$ have been demonstrated up to 4 GHz modulation frequency [67Kam].

7.1.3.3.1.3 Crystal class $\bar{4}3m$

Examples of this group are InAs, CuCl, ZnS, GaAs, and CdTe, which are due to the cubic crystal class naturally isotropic. The last two kinds of crystals are used for modulation in the infrared, since they remain transparent beyond 10 μm. The three non-vanishing electro-optic tensor elements are r_{41}, $r_{52} = r_{41}$, and $r_{63} = r_{41}$.

Longitudinal modulator, z-cut: In the presence of an electric field in z direction the index ellipsoid becomes using (7.1.4)

$$\frac{x^2}{n^2} + \frac{y^2}{n^2} + \frac{z^2}{n^2} + 2r_{41}xyE_z = 1 \ .$$

The principal dielectric axes x and y are rotated around the z-axis by 45°. The new index ellipsoid in principle coordinate system (x', y', z') becomes

$$\left(\frac{1}{n^2} + r_{41}E_z\right) \cdot x'^2 + \left(\frac{1}{n^2} - r_{41}E_z\right) \cdot y'^2 + \frac{z'^2}{n^2} = 1 \ ,$$

and the principal indices of refraction are $n_{x'} = n - \frac{1}{2}n^3 r_{41} E_z$, $n_{y'} = n + \frac{1}{2}n^3 r_{41} E_z$ and $n_{z'} = n$. This crystal cut is used in a longitudinal modulator.

In case of a Phase Modulator (PM), the light must be polarized either in x' or y' direction, giving an electrically induced phase change of $\Delta\Phi = \frac{\pi}{\lambda} \cdot n^3 r_{41} V$ resulting in a half-wave voltage of $V_\pi = \lambda/(n^3 r_{41})$ (PM).

For Amplitude Modulation (AM) the front polarizer can be aligned along the x-axis so that equal amplitudes of the x' and y' modes are exited. The phase retardation results in $\Gamma = \frac{2\pi}{\lambda} \cdot n^3 r_{41} V$ giving a half-wave voltage of $V_\pi = \lambda/[2(n^3 r_{41})]$ (AM).

Transverse modulation: For transverse modulation the field must be applied along a cube diagonal direction and the crystal must be cut appropriately. E.g. in case of a field oriented in $\langle 110 \rangle$ direction and having a magnitude of $E_x = E_y = \frac{1}{\sqrt{2}} \cdot E$ it results in $n_{x'} = n + \frac{1}{2}n^3 r_{41} E$, $n_{y'} = n - \frac{1}{2}n^3 r_{41} E$ and $n_{z'} = n$. The obtained phase retardation is $\Gamma = \frac{2\pi}{\lambda} \cdot n^3 r_{41} \cdot \frac{L}{d} \cdot V$ and the half-wave voltage is given by $V_\pi = \frac{d}{L} \cdot \frac{\lambda}{2(n^3 r_{41})}$.

Data of phase retardation and electro-optical properties of $\bar{4}$3m crystals for a field along directions $\langle 001 \rangle$, $\langle 110 \rangle$, or $\langle 111 \rangle$ are found in [61Nam, 84Yar].

7.1.3.3.2 Selected electro-optic materials and modulator systems

In Table 7.1.1 selected electro-optic materials and their properties are presented.

KDP and its isomorphic single crystal KD*P are widely used for electro-optic Q-switches in Nd:YAG-, Nd:YLF-, Ti:sapphire-, and alexandrite lasers. The damage threshold of these crystals of about 10 GW/cm^2 ($<$ 500 ps) is very high. The longitudinal half-wave voltage at $\lambda = 0.546$ μm is 7.65 kV for KDP and 2.98 kV for KD*P, respectively.

$LiNbO_3$ is also used for these applications, mostly in transverse modulators. The half-wave voltage is below 1 kV, but the damage threshold is only in the range of 250 MW/cm^2.

In Table 7.1.2 performances of some commercially available EO modulators with driver electronics are listed. EO modulator systems are available from a number of different suppliers. Among these are in alphabetic order and without claim of completeness: Agere-Systems, Conoptics, Cy-Optics, e2v technologies, Electro-Optical Products Corp., EOSPACE, Fujitsu, Gsaenger, IPAG-Innovative, JDS Uniphase, Lasermetrics, Lucent Technologies, New Focus, Nova Phase, Sciro, Sumitomo, and Quantum Technology. Many others may exist and can be found in the net, e.g. via `www.globalspec.com`. Devices exemplarily listed in Table 7.1.2 may also be offered by other suppliers with similar or even superior features. Especially, high-speed modulators for telecommunication system applications, as shown for one example in the Table's last row, can operate up to data rates of 40 Gbit/s and beyond at rather low drive voltages. 0.9 V drive voltage at 40 Gbit/s for a $LiNbO_3$ EO modulator has been demonstrated at Fujitsu Laboratories in 2002.

7.1.3.4 Electro-optic beam deflector

The electro-optic effect is also used to deflect light beams. A simple realization of such a deflector using e.g. a KDP crystal is shown in Fig. 7.1.5 [75Yar]. It consists of two KDP prisms with edges along the x', y', and z directions having their z-axes opposite to one another but are otherwise similarly oriented. The electric field is applied along z and the light propagates in the y' direction with its polarization along x'. The index of refraction "seen" by ray A, which propagates entirely in the upper prism, is given as $n_A = n_o - \frac{n_o^3}{2} \cdot r_{63} E_z$, while in the lower prism with opposite field direction with respect to the z-axis, ray B "sees" $n_B = n_o + \frac{n_o^3}{2} \cdot r_{63} E_z$. The deflection angle comes out as

Table 7.1.1. Selected Electro-Optic (EO) materials and their properties [79Coo, 84Yar, 86Kam].

Material	Symmetry	Wavelength λ [μm]	EO-coefficient r_{ik} [10^{-12} m/V]	Index of refraction n	Figure of merit $n^3 r$ [10^{-12} m/V]	Dielectric constant ε_i
CdTe	$\bar{4}$3m	1.0	(T) $r_{41} = 4.5$	$n = 2.84$	103	(S) 9.4
		10.6	(T) $r_{41} = 6.8$	$n = 2.60$	120	
GaAs	$\bar{4}$3m	1.15	(T) $r_{41} = 1.43$	$n = 3.43$	58	(T) 12.3
		10.6	(T) $r_{41} = 1.51$	$n = 3.3$	54	
GaP	$\bar{4}$3m	0.55–1.5	(T) $r_{41} = -1.0$	$n = 3.66$–3.08		(S) 10
		0.633	(S) $r_{41} = -0.97$	$n = 3.32$	35	
$\beta-$ZnS	$\bar{4}$3m	0.633	(S) $r_{41} = -1.6$	$n = 2.35$		
ZnSe	$\bar{4}$3m	0.633	(S) $r_{41} = 2.0$	$n = 2.60$	35	(S) 9.1
		10.6	(T) $r_{41} = 2.2$	$n = 2.39$	30	
ZnTe	$\bar{4}$3m	0.633	(T) $r_{41} = 4.04$	$n = 2.99$	108	(S) 10.1
		10.6	(T) $r_{41} = 3.9$	$n = 2.70$	77	
KDP (KH_2PO_4)	$\bar{4}$2m	0.546	(T) $r_{41} = 8.77$	$n_o = 1.5115$		(T) $\varepsilon_1 = \varepsilon_2 = 42$
			(T) $r_{63} = 10.3$	$n_e = 1.4698$		(T) $\varepsilon_3 = 21$
		0.633	(T) $r_{41} = 8.0$	$n_o = 1.5074$		(S) $\varepsilon_1 = \varepsilon_2 = 44$
			(T) $r_{63} = 11$	$n_e = 1.4669$		(S) $\varepsilon_3 = 21$
KD*P (KD_2PO_4)	$\bar{4}$2m	0.546	(T) $r_{41} = 8.8$	$n_e = 1.4683$		(S) $\varepsilon_1 = \varepsilon_2 = 58$
			(T) $r_{63} = 26.4$	$n_o = 1.5079$		(T) $\varepsilon_3 = 50$
		0.633	(T) $r_{63} = 24.1$	$n_o = 1.502$		(S) $\varepsilon_3 = 48$
				$n_e = 1.462$		
ADP ($NH_4H_2PO_4$)	$\bar{4}$2m	0.546	(T) $r_{41} = 23.76$	$n_o = 1.5266$		(T) $\varepsilon_1 = \varepsilon_2 = 56$
			(T) $r_{63} = 8.56$	$n_e = 1.4808$		(T) $\varepsilon_3 = 15$
		0.633	(T) $r_{41} = 23.41$	$n_o = 1.5220$		(S) $\varepsilon_1 = \varepsilon_2 = 58$
			(T) $r_{63} = 8.8$	$n_e = 1.4773$		(S) $\varepsilon_3 = 14$
$LiNbO_3$	3m	0.633	(T) $r_{13} = 9.6$ (S) $r_{13} = 8.6$	$n_o = 2.286$		(T) $\varepsilon_1 = \varepsilon_2 = 78$
			(T) $r_{22} = 6.8$ (S) $r_{22} = 3.4$	$n_e = 2.200$		(T) $\varepsilon_3 = 32$
			(T) $r_{33} = 30.9$ (S) $r_{33} = 30.8$			(S) $\varepsilon_1 = \varepsilon_2 = 43$
			(T) $r_{51} = 32.6$ (S) $r_{51} = 28$			(S) $\varepsilon_3 = 28$
$LiTaO_3$	3m	0.633	(T) $r_{13} = 8.4$ (S) $r_{13} = 7.5$	$n_o = 2.176$		(T) $\varepsilon_1 = \varepsilon_2 = 51$
			(T) $r_{22} = -0.2$ (S) $r_{22} = 1$	$n_e = 2.180$		(T) $\varepsilon_3 = 45$
			(T) $r_{33} = 30.5$ (S) $r_{33} = 33$			(S) $\varepsilon_1 = \varepsilon_2 = 41$
			(S) $r_{51} = 20$			(S) $\varepsilon_3 = 43$

(T): low frequency from dc through audio range; (S): high frequency.

$$\theta = \frac{L \cdot (n_B - n_A)}{d} = \frac{L}{d} \cdot n_o^3 r_{63} E_z \; . \tag{7.1.16}$$

To get the number of resolvable spots, N, it is assumed that the crystal is placed at the waist of a Gaussian beam with spot diameter $\bar{d}$. The far-field beam divergence is $\theta_{\text{beam}} = 2\lambda/(\pi n \bar{d})$. Taking $d = \bar{d}$ and $n \approx 1$ (in air) the maximum number of resolvable spots is

$$N = \frac{\theta}{\theta_{\text{beam}}} = \frac{\pi}{2\lambda} \cdot L n_o^3 r_{63} E_z \; . \tag{7.1.17}$$

An electric field that induces a birefringent retardation (in the distance L) of $\Delta\Gamma = \pi$ will yield $N = 1$.

Table 7.1.2. Performances of some commercially available EO modulators with driver electronics.

Supplier	Crystal	Spectral range $\Delta\lambda$ [nm]	Aperture diameter [mm]	Contrast at wavelength	Half-wave voltage V_π at wavelength	Operating frequency (−3 dB-limit)
Conoptics	ADP	300...750	3.5	500 : 1 at 633 nm	263 V at 500 nm	1...125 MHz
Conoptics	KD*P	300...1100	3.1	700 : 1 at 1064 nm	482 V at 1064 nm	1...200 MHz
Quantum Technology	$LiTaO_3$	800...2500	1	100 : 1 at 633 nm	107 V at 633 nm	DC... 1 GHz
New Focus	MgO:$LiNbO_3$	500...1600	1	> 100 : 1 at 1 µm	45...79 V at 1 µm	2.0...4.6 GHz
New Focus	MgO:$LiNbO_3$	500...1600	1×2 mm^2	> 100 : 1 at 1 µm	79 V at 1 µm	6.8 or 9.2 GHz
Fujitsu	$LiNbO_3$	1530...1570	fiber-coupled	> 100 : 1 at 1550 nm	5 V at 1550 nm	DC... 30 GHz

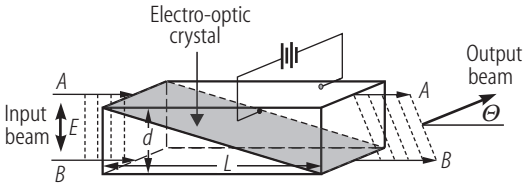

Fig. 7.1.5. Double-prism electro-optic beam deflector.

7.1.4 Kerr electro-optic effect modulators

The first ever investigated electro-optic effect is named after the Scottish physicist John Kerr (1824–1907) who discovered it in the year 1875. He found that an isotropic transparent substance becomes birefringent when placed in an electric field. The quadratic electro-optic effect is a higher-order effect and is normally neglected when the linear electro-optic effect is present. Unlike the linear effect, it exists in a medium with any symmetry. An electric field, in general, changes the dimension and orientation of the index ellipsoid. This change is dependent upon the direction of the applied electric field as well as the 6×6 matrix elements s_{ij}, see text below (7.1.2).

The equation of the index ellipsoid in the presence of an electric field can be written

$$\left(\frac{1}{n_x^2} + s_{1j}\xi_j^2\right)x^2 + \left(\frac{1}{n_y^2} + s_{2j}\xi_j^2\right)y^2 + \left(\frac{1}{n_z^2} + s_{3j}\xi_j^2\right)z^2 + 2yzs_{4j}\xi_j^2 + 2zxs_{5j}\xi_j^2 + 2xys_{6j}\xi_j^2 = 1\ , \tag{7.1.18}$$

where $\xi_1^2, \ldots, \xi_6^2 = E_x^2,\ E_y^2,\ E_z^2,\ 2E_yE_z,\ 2E_zE_x,\ 2E_xE_y$.

A table containing the form of the quadratic electro-optic coefficients is given in [67Nye, 84Yar]. Extensive tables of quadratic electro-optic coefficients are listed in [79Coo].

7.1.4.1 Kerr effect in isotropic media

An optically isotropic medium placed in a static electric field becomes birefringent. This effect is associated mostly with the alignment of the molecules in the presence of the field. The medium

then gains optically uniaxial anisotropy where the electric field defines the optical axis. Choosing an electric field E along the z-axis of an isotropic crystal the index ellipsoid becomes

$$\left(\frac{1}{n^2}+s_{12}E_z^2\right)x^2+\left(\frac{1}{n^2}+s_{12}E_z^2\right)y^2+\left(\frac{1}{n^2}+s_{11}E_z^2\right)z^2=1\ , \tag{7.1.19}$$

where $s_{13}=s_{23}=s_{12}$ and $s_{33}=s_{11}$ have been used. Further, for isotropic media $s_{44}=s_{55}=s_{66}=\frac{1}{2}(s_{11}-s_{12})$. This index ellipsoid can be written in a more compact form as

$$\frac{\left(x^2+y^2\right)}{n_\mathrm{o}^2}+\frac{z^2}{n_\mathrm{e}^2}=1 \tag{7.1.20}$$

using $n_\mathrm{o}=n-\frac{1}{2}n^3s_{12}E^2$ and $n_\mathrm{e}=n-\frac{1}{2}n^3s_{11}E^2$. The birefringence becomes $n_\mathrm{e}-n_\mathrm{o}=\frac{1}{2}n^3(s_{12}-s_{11})E^2=-n^3s_{44}E^2$. According to empirical results the Kerr birefringence is often written as $n_\mathrm{e}-n_\mathrm{o}=K\lambda E^2$, where K is the so-called Kerr constant and λ is the vacuum wavelength. Kerr constant and quadratic electro-optic coefficients in isotropic media are, therefore, related by $s_{44}=-K\lambda/n^3$. Table 7.1.3 lists Kerr constants of several liquids used in Kerr modulator devices. Table 7.1.4 lists some selected quadratic electro-optic coefficients.

Table 7.1.3. Kerr constants for some selected liquids at 20°C [84Yar].

Substance		Wavelength λ [μm]	Index of refraction n	Kerr constant K [m/V^2]
Benzene	C_6H_6	0.546	1.503	4.9×10^{-15}
		0.633	1.496	4.14×10^{-15}
Carbon disulfide	CS_2	0.546	1.633	3.88×10^{-14}
		0.633	1.619	3.18×10^{-14}
		0.694	1.612	2.83×10^{-14}
		1.000	1.596	1.84×10^{-14}
		1.600	1.582	1.11×10^{-14}
Chloroform	$CHCl_3$	0.589		-3.5×10^{-14}
Water	H_2O	0.589		5.1×10^{-14}
Nitrotoluene	$C_5H_7NO_2$	0.589		1.37×10^{-12}
Nitrobenzene	$C_6H_5NO_2$	0.589		2.44×10^{-12}

Table 7.1.4. Some selected quadratic electro-optic coefficients [79Coo].

Substance	Symmetry	Wavelength λ [μm]	Electro-optic coefficients $n_\mathrm{o}^3 s_{ij}$ [10^{-18} m^2/V^2]	Index of refraction n
$BaTiO_3$	m3m	0.500	$n_\mathrm{o}^3(s_{11}-s_{12})=72,000$ $n_\mathrm{o}^3 s_{44}=44,000$ near $T_\mathrm{c}=120$°C	$n_\mathrm{o}=2.42$
$KTa_{0.65}Nb_{0.35}O_3$	m3m	0.633	$n_\mathrm{o}^3(s_{11}-s_{12})=34,700$ at 20°C	$n_\mathrm{o}=2.29$
$Pb_{0.93}La_{0.07}(Zr_{0.65}Ti_{0.35})0_3$	∞m	0.550	$n_\mathrm{o}^3(s_{33}-s_{13})=26,000$ near $T_\mathrm{c}=63$°C	$n_\mathrm{o}=2.450$

A Kerr modulator consists of a glass cell containing two transverse electrodes that is filled with a polar liquid and placed between crossed linear polarizers whose transmission axes are at $\pm 45°$ to the applied electric field. The great value of such a device lies in the fact that it can respond effectively to frequencies up to 10 GHz. Kerr cells, usually containing nitrobenzene or carbon disulfide, have for many years been used as Q-switches in pulsed laser systems. A cell of length L and electrode distance d gives a retardation of

$$\Gamma = 2\pi \cdot KL \cdot \frac{V^2}{d^2} \; . \tag{7.1.21}$$

A typical nitrobenzene cell where $d = 1$ cm and L is several cm will require a voltage in the order of 3×10^4 V to respond as a half-wave plate. A drawback is that nitrobenzene is both poisonous and explosive. Therefore, transparent solids like the crystals KTN ($KTa_{0.65}Nb_{0.35}O_3$), barium titanate ($BaTiO_3$), or PLZT ($Pb_{0.93}La_{0.07}(Zr_{0.65}Ti_{0.35})0_3$) e.g. are of interest for such modulators.

7.1.5 Acousto-optic modulators

An acoustic wave propagating in an optically transparent medium produces a periodic modulation of the index of refraction via the elasto-optic effect. This provides a moving phase grating which may diffract portions of an incident light into one or more directions. This phenomenon, known as the acousto-optic diffraction, has led to a variety of optical devices that perform spatial, temporal, and spectral modulation of light. Acousto-optic devices are used in laser applications for electronic control of the intensity or position of a laser beam.

Acoustic waves in solids can appear as longitudinal or transverse (shear) waves, whereas in liquids and gases only longitudinal waves are possible. The acousto-optic interaction is very similar to that of electro-optic modulation, except that in the acousto-optic interaction an RF field is required in any case. A number of different useful materials, such as SiO_2, TeO_2, $LiNbO_3$, $PbMoO_4$, have been exploited for fabrication of acousto-optic modulator devices.

7.1.5.1 The photoelastic effect

The photoelastic effect in a material causes coupling of mechanical strain to the optical index of refraction. This effect occurs in all states of matter and is commonly described by the change in the optical impermeability tensor. Using contracted indices the relation is [86Got]

$$\Delta \left(\frac{1}{n^2}\right)_i = p_{ij} S_j \; , \quad i,j = 1,2,\ldots,6 \; ,$$

where p_{ij} are the strain-optic coefficients and S_j are the strain components.

The equation of the index ellipsoid in the presence of strain can then be written as

$$\left(\frac{1}{n_x^2} + p_{1j}S_j\right) x^2 + \left(\frac{1}{n_y^2} + p_{2j}S_j\right) y^2 + \left(\frac{1}{n_z^2} + p_{3j}S_j\right) z^2 + 2yzp_{4j}S_j + 2zxp_{5j}S_j + 2xyp_{6j}S_j = 1 \; , \tag{7.1.22}$$

where n_x, n_y, n_z are the principal indices of refraction and p_{ij} are defined in the principal coordinate system. Again summation over repeated indices is assumed.

As an example a longitudinal sound wave is considered propagating along the z direction of an isotropic medium (e.g. water). For a sinusoidal particle displacement $\boldsymbol{u}(z,t) = A\,\bar{\boldsymbol{z}}\cos(\Omega t - Kz)$ with amplitude A, sound frequency Ω, and wave number $K = 2\pi/\Lambda$ the associated strain field is

$$S_3 = KA \cdot \sin(\Omega t - Kz) = S \cdot \sin(\Omega t - Kz) \ . \tag{7.1.23}$$

For an isotropic medium, the relevant elasto-optic coefficients are [84Yar]: $p_{13} = p_{23} = p_{12}$, $p_{33} = p_{11}$, and $p_{43} = p_{53} = p_{63} = 0$. The new index ellipsoid results in

$$\left(\frac{1}{n^2} + p_{12}S \cdot \sin(\Omega t - Kz)\right) x^2 + \left(\frac{1}{n^2} + p_{12}S \cdot \sin(\Omega t - Kz)\right) y^2 + \left(\frac{1}{n^2} + p_{11}S \cdot \sin(\Omega t - Kz)\right) z^2 = 1 \ . \tag{7.1.24}$$

Here no mixed terms are involved and the principal axes remain unchanged. The new principal indices of refraction are

$$n_x = n - \frac{1}{2}n^3 p_{12} S \cdot \sin(\Omega t - Kz) \ ,$$
$$n_y = n - \frac{1}{2}n^3 p_{12} S \cdot \sin(\Omega t - Kz) \ ,$$
$$n_z = n - \frac{1}{2}n^3 p_{11} S \cdot \sin(\Omega t - Kz) \ .$$

The medium now carries a volume-index (phase) grating with grating constant $K = 2\pi/\Lambda$ that travels at speed $v = \Omega/K$.

Another example may be a sound wave along the $\langle 001 \rangle$ direction (z-axis) in a cubic crystal of symmetry m3m (e.g. germanium). Considering a shear wave polarized in $\langle 010 \rangle$ direction (y-axis) with particle displacement $\boldsymbol{u}(z,t) = A\,\bar{\boldsymbol{y}}\cos(\Omega t - Kz)$, the strain field associated with this shear comes out to be

$$S_4 = KA \cdot \sin(\Omega t - Kz) = S \cdot \sin(\Omega t - Kz) \ . \tag{7.1.25}$$

According to the relevant elasto-optic coefficients for the point group symmetry m3m $p_{14} = p_{24} = p_{34} = p_{54} = p_{64} = 0$, $p_{44} \neq 0$ the index ellipsoid thus becomes [84Yar]

$$\frac{x^2 + y^2 + z^2}{n^2} + 2yz \cdot p_{44} S \cdot \sin(\Omega t - Kz) = 1 \ . \tag{7.1.26}$$

The new principal axes are obtained by rotating the coordinates around the x-axis by 45°, and the new principal indices of refraction are given by

$$n_{x'} = n \ ,$$
$$n_{y'} = n - \frac{1}{2}n^3 p_{44} S \sin(\Omega t - Kz) \ ,$$
$$n_{z'} = n + \frac{1}{2}n^3 p_{44} S \sin(\Omega t - Kz) \ .$$

As before, a moving optical volume-index grating is excited from the shear acoustic wave via the strain-optic effect.

The forms of the elasto-optic coefficients are identical to those for the quadratic electro-optic effect [67Nye, 84Yar]. Tables of elasto-optic coefficients p of various materials are found e.g. in [72Pin, 79Hel, 86Got].

7.1.5.2 Interaction regimes

The quantity of the factor $Q = (2\pi\lambda L)/(n\Lambda^2)$ determines the interaction of light with sound waves. Herein λ is the vacuum wavelength of light, n is the refractive index of the medium, L is the distance the light travels through the acoustic wave, and Λ is the acoustic wavelength [67Kle].

7.1.5.2.1 Raman–Nath regime

$Q \ll 1$: The approximation holds for $L \ll (n\Lambda^2)/(2\pi\lambda)$. The laser beam may be incident roughly normal to the acoustic beam. Then several diffraction orders appear distinguished by the numbers $-m, \ldots, -2, -1, 0, 1, 2, \ldots, m$ at diffraction angels according to $\sin\theta_m = m\lambda/n\Lambda$ with corresponding frequencies $\omega - m\Omega$, $\ldots$, $\omega - 2\Omega$, $\omega - \Omega$, ω, $\omega + \Omega$, $\omega + 2\Omega$, $\ldots$, $\omega + m\Omega$, see Fig. 7.1.6.

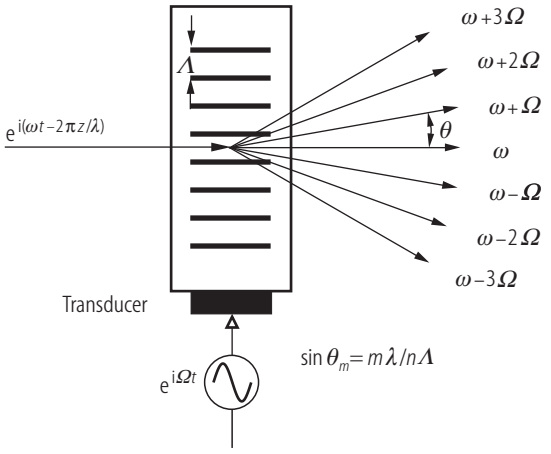

Fig. 7.1.6. Raman–Nath diffraction of light into multiple orders.

The intensities are given by Bessel functions J_m. The diffraction efficiency of the mth-order Raman–Nath diffraction is thus given by

$$\eta = J_m^2(\beta) = J_m^2(kL\Delta n) \ , \tag{7.1.27}$$

where Δn is the change in refractive index caused by the acoustic wave. The diffraction efficiency of order ± 1 is maximum when the modulation index is $\beta = 1.85$. The zeroth order is completely quenched when $\beta = 2.4$, because of $J_0(2.4) = 0$. For small values of β it results in [86Got]

$$\frac{I_1}{I_0} = \beta^2 = \frac{\pi^2}{2} \cdot \left(\frac{L}{\lambda}\right)^2 M_2 I_\mathrm{a} \ , \quad \text{where} \quad M_2 = \frac{n^6 p^2}{\rho v^3} \ . \tag{7.1.28}$$

Here ρ is the mass density and I_a is the acoustic intensity. If the RF sound carrier is modulated with an information-bearing signal, the modulation of the diffracted light will be reasonably linear provided β is less than 2.4. The main disadvantage of operating in the Raman–Nath regime is the small interaction length and the excessive acoustic power required.

Therefore, most acousto-optic devices operate in the Bragg regime; the common exception being acousto-optic mode lockers.

7.1.5.2.2 Bragg regime

$Q \gg 1$: The approximation holds for $L \gg (n\Lambda^2)/(2\pi\lambda)$. The physical properties can be treated, for instance, by coupled-mode theory. It shows up that at one particular angle of incidence θ_B of a laser beam only one diffraction order is produced by constructive interference in the interaction region, possible other orders are annihilated by destructive interference. This can be understood as a resonant reflection of light from the acoustic wave. A convenient description can be given for light and sound waves as colliding photons and phonons governed by the laws of conservation of energy and momentum. Momentum conservation requires

$$k_d = k_i + K \ , \tag{7.1.29}$$

where

$k_i = 2\pi n/\lambda$: wave vector of incident light beam,
$k_d = 2\pi n/\lambda$: wave vector of diffracted light beam,
$K = 2\pi/\Lambda = 2\pi f/v$: wave vector of acoustic wave.

Conservation of energy takes the form $\omega_d = \omega_i \pm \Omega$.

Different materials and a variety of configurations can be used for modulation. These can be described by terms such as longitudinal- and shear-mode, isotropic and anisotropic. While these all rely on the basic principles of momentum and energy conservation, different modes of operation have very different performances.

7.1.5.2.2.1 Isotropic interaction

In an isotropic interaction incident and diffracted light beams see the same refractive index in the crystal. There is no change in polarization associated with the interaction. These interactions usually occur in liquids, in homogenous crystals, or in birefringent crystals suitably cut, see Fig. 7.1.7.

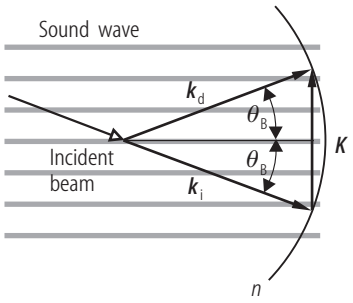

Fig. 7.1.7. Bragg diffraction in an isotropic medium.

If θ is the angle between the incident or diffracted beam and the acoustic wavefront, the momentum conservation yields for Bragg condition

$$K = 2k \cdot \sin\theta_B \quad \text{or} \quad 2\Lambda \cdot \sin\theta_B = \frac{\lambda}{n} \ . \tag{7.1.30}$$

The separation angle between first and zeroth order is twice the angle of incidence and, therefore, twice the Bragg angle. In practice, the Bragg angle is often small and can be written as

$$\theta_B = \frac{\lambda}{2n\Lambda} = \frac{\lambda f}{2nv} \ . \tag{7.1.31}$$

7.1.5.2.2.2 Anisotropic interaction

The refractive index in an optically anisotropic medium such as a birefringent crystal depends on the direction as well as the polarization of the light beam. In general, the refractive indices of the incident and diffracted light beams are different.

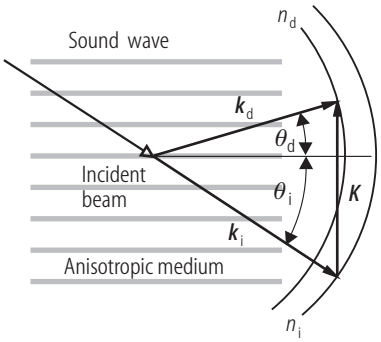

Fig. 7.1.8. Bragg diffraction in an anisotropic medium.

From the wave vector diagram shown in Fig. 7.1.8 one obtains [95Cha]

$$\sin\theta_\mathrm{i} = \frac{\lambda}{2n_\mathrm{i}\Lambda}\cdot\left[1+\frac{\Lambda^2}{\lambda^2}\left(n_\mathrm{i}^2-n_\mathrm{d}^2\right)\right] ,$$
$$\sin\theta_\mathrm{d} = \frac{\lambda}{2n_\mathrm{d}\Lambda}\cdot\left[1-\frac{\Lambda^2}{\lambda^2}\left(n_\mathrm{i}^2-n_\mathrm{d}^2\right)\right] . \qquad (7.1.32)$$

Notice that the first term on the right-hand side of these equations is the same as for the isotropic case, while the remaining terms denote the modification due to the effect of anisotropy. This significantly changes the angle/frequency characteristics of acousto-optic diffraction.

As an example, Bragg diffraction in a positive uniaxial crystal (e.g. $LiNbO_3$) is considered. An incident extraordinary wave polarized parallel to the c-axis with refractive index n_e is diffracted into an ordinary wave polarized perpendicular to the c-axis with refractive index n_o. Then, θ_i and θ_d are both functions of λ/Λ. Bragg diffraction is only possible when $|n_\mathrm{o}-n_\mathrm{e}| \le \lambda/\Lambda \le |n_\mathrm{o}+n_\mathrm{e}|$. In the small angle approximation, the separation angle between first and zeroth order is nearly the same as in the case of isotropic diffraction.

For acousto-optic modulators and acousto-optic deflectors, optical birefringence in principle is not necessary. However, it is a requirement for materials used in acousto-optic tunable filters.

7.1.5.2.2.3 Efficiency

Using coupled-mode theory the fraction of power of an incident light beam transferred into the diffracted beam after traveling a distance L is for validity of the Bragg condition

$$\frac{I_\mathrm{d}}{I_\mathrm{i}} = \sin^2(\kappa L) , \qquad (7.1.33)$$

where κ is a coupling constant. A slight deviation from the Bragg condition caused by a wave vector mismatch Δk results in

$$\frac{I_\mathrm{d}}{I_\mathrm{i}} = (\kappa L)^2\cdot\mathrm{sinc}^2\left[(\kappa L)^2+\left(\frac{L\Delta k}{2}\right)^2\right]^{\frac{1}{2}} , \qquad (7.1.34)$$

where $\mathrm{sinc}(x) = \sin(x)/x$. The mismatch Δk can be caused either by misalignment of the laser beam or by distortion of the acoustic wavefront due to the finite size of the transducer [84Yar].

The coupling constant κ can be expressed in terms of the strain components and the elasto-optic coefficients of the material. The efficiency for Bragg diffraction according to (7.1.33) results in

$$\eta = \frac{I_\mathrm{d}}{I_\mathrm{i}} = \sin^2\left(\frac{\pi n^3}{2\lambda_0 \cos\theta_\mathrm{B}} \cdot pSL\right) , \tag{7.1.35}$$

where pS are the matrix elements $p_{ij}S_j$. The strain acoustic amplitude S is related to the acoustic intensity I_a by $S = [2I_\mathrm{a}/(\rho v^3)]^{\frac{1}{2}}$, where ρ is the mass density and v is the velocity of sound in the crystal.

A homogeneously excited transducer of height H, width L, and acoustic power P_a yields $I_\mathrm{a} = P_\mathrm{a}/(HL)$. Combining these relations it gives

$$\eta = \frac{I_\mathrm{d}}{I_\mathrm{i}} = \sin^2\left\{\frac{\pi}{\sqrt{2}\,\lambda_0 \cos\theta_\mathrm{B}} \cdot \left[M_2 P_\mathrm{a} \cdot \left(\frac{L}{H}\right)\right]^{\frac{1}{2}}\right\} , \tag{7.1.36}$$

where $M_2 = n^6 p^2/(\rho v^3)$ is a figure of merit for judging the usefulness of a material with respect to efficiency.

For small acoustic power levels, the diffraction efficiency is thus linearly proportional to the acoustic power

$$\eta = \frac{\pi^2}{2\lambda_0^2 \cos^2\theta_\mathrm{B}} \cdot \left[M_2 P_\mathrm{a} \cdot \left(\frac{L}{H}\right)\right] , \tag{7.1.37}$$

which is the basis of an acousto-optic modulator. This approximation is valid when the peak efficiency is below 70 %. The acoustic power required for 100 % modulation (i.e. total conversion of the incident light) is given by

$$P_\mathrm{a} = \frac{\lambda_0^2 \cos^2\theta_\mathrm{B}}{2M_2} \cdot \left(\frac{H}{L}\right) . \tag{7.1.38}$$

Therefore, according to (7.1.37) a small aspect ratio (H/L) is desirable for an efficient operation of a modulator.

7.1.5.2.2.4 Bandwidth

A modulated acoustic wave is defined by its center frequency f_0 and modulation bandwidth Δf. The attainable modulation bandwidth Δf of an acousto-optic modulator results from the angular spread of the beams of light and sound. For finite beams of light and sound in a modulator a relation of Bragg angle change $\Delta\theta$ and acoustic frequency change Δf comes out as

$$\Delta f = \frac{2nv \cdot \cos\theta}{\lambda} \cdot \Delta\theta . \tag{7.1.39}$$

The angle of incidence covers a range of $\Delta\theta = \delta\theta_\mathrm{o} + \delta\theta_\mathrm{a}$, where $\delta\theta_\mathrm{o}$ and $\delta\theta_\mathrm{a}$ are the angular spread of light wave vector and sound wave vector, respectively. The diffracted light beam for each fixed angle of incident light has an angular spread into sidebands of $2\delta\theta_\mathrm{a}$, see Fig. 7.1.9. Each direction corresponds to a different frequency shift. In order to recover best the intensity modulation of the diffracted light beam, mixing the spectrally shifted components collinearly in a square-law detector is necessary, for optimum condition $\delta\theta_\mathrm{o} \approx \delta\theta_\mathrm{a} = \frac{1}{2}\Delta\theta$.

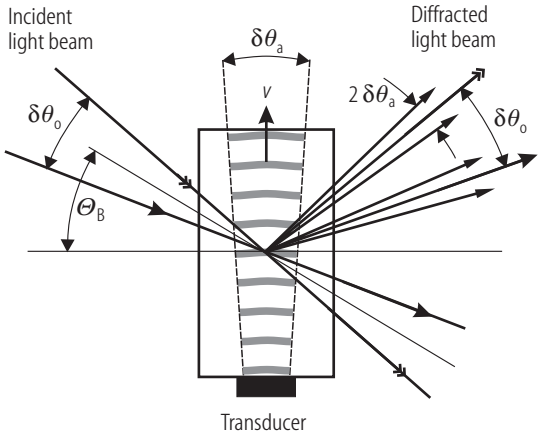

Fig. 7.1.9. Diffraction geometry of a Bragg acousto-optic modulator.

In most practical cases the incident laser beam is a focused Gaussian beam with beam waist diameter $\bar{d}$. The corresponding optical beam divergence is $\Delta\theta = 4\lambda/(\pi n\bar{d})$. Then, taking $\delta\theta = \frac{1}{2}\Delta\theta$ it yields

$$(\Delta f)_{\mathrm{m}} = \frac{1}{2}\Delta f = \frac{2}{\pi}\cdot\frac{v}{\bar{d}}\cdot\cos\theta \approx \frac{1}{\tau}\,, \tag{7.1.40}$$

where $\tau = \bar{d}/v$ is the acoustic transit time across the optical aperture [95Cha]. Thus, the modulation bandwidth is roughly equal to the reciprocal of the acoustic transit time across the optical beam. The maximum fractional bandwidth of an acousto-optic modulator is usually determined by the condition that the diffracted beam does not interfere with the undiffracted beam, i.e. $\Delta\theta < \theta_{\mathrm{B}}$. Then, one obtains from (7.1.39) and the relation $\theta_{\mathrm{B}} = \lambda f/2nv$ (7.1.31), and when assuming $\Delta\theta \approx \Delta\theta_{\mathrm{B}}$ for the maximum modulation bandwidth

$$\frac{(\Delta f)_{\mathrm{m}}}{f} \approx \frac{\Delta f}{2f} \leq \frac{1}{2}\,. \tag{7.1.41}$$

Thus, the maximum modulation bandwidth is approximately one-half of the acoustic frequency. Therefore, large modulation bandwidths are only available with high-frequency Bragg diffraction.

A useful figure of merit [66Gor], including the modulator bandwidth Δf and the center acoustic frequency f_0 and being independent of the modulator width L, is:

$$2\eta f_0\Delta f = M_1\cdot\frac{2\pi^2}{\lambda_0^3\cos\theta_{\mathrm{B}}}\cdot\left(\frac{P_{\mathrm{a}}}{H}\right) \quad \text{with} \quad M_1 = \frac{n^7p^2}{\rho v}\,. \tag{7.1.42}$$

Another quantity [67Dix], which is independent of the acoustic and optical beam dimensions, is

$$\eta f_0 = M_3\cdot\frac{\pi^2}{2\lambda_0^3\cos^2\theta_{\mathrm{B}}}\cdot P_{\mathrm{a}} \quad \text{with} \quad M_3 = \frac{n^7p^2}{\rho v^2}\,. \tag{7.1.43}$$

Values of M_1, M_2, and M_3 for a number of materials are listed in Table 7.1.5.

Another important material parameter is the acoustic attenuation that limits the center frequency, bandwidth, and useful aperture of acousto-optic devices. Following the theory the dominant contribution to acoustic attenuation in crystals is caused by relaxation of the thermal phonon distribution toward equilibrium. A widely used result of this theory is the relation derived by Woodruff and Ehrenreich [61Woo], which shows that the acoustic attenuation increases quadratically with frequency. Commonly the acoustic attenuation is given in units of dB per microsecond of acoustic propagation time and GHz^2, i.e. $\mathrm{dB}/(\mu\mathrm{s}\cdot\mathrm{GHz}^2)$, see Table 7.1.5.

Table 7.1.5 lists relevant properties of selected acousto-optic materials. The listed figures of merit are normalized relative to that of fused silica which has the following absolute values: $M_1 = 7.83\times10^{-8}\ \mathrm{m^2sKg^{-1}}$, $M_2 = 1.51\times10^{-15}\ \mathrm{s^3Kg^{-1}}$, $M_3 = 1.3\times10^{-13}\ \mathrm{m^2s^2Kg^{-1}}$.

Table 7.1.5. Selected acousto-optic materials [72Kor, 86Got, 95Cha].

Material	Optical transmission T [μm]	Density ρ [g/cm^3]	Acoustic mode	Acoustic velocity v [mm/μs]	Acoustic attenuation α_a [dB/(μs · GHz^2)]	Optical polarization	Refractive index n	Figures of merit (relative to fused quartz)		
								M_1	M_2	M_3
Fused silica	0.2...4.5	2.2	L	5.96	7.2	⊥	1.46	1.0	1.0	1.0
$LiNbO_3$	0.4...4.5	4.64	L[100]	6.57	1.0	35° Y Rot.	2.2	8.5	4.6	7.7
			S(100)35°	∼ 3.6	∼ 1.0	[100]	2.2	2.3	4.2	3.8
TiO_2	0.45...6.0	4.23	L[110]	7.93	1.0	⊥	2.58	18.6	6.0	14
$PbMoO_4$	0.42...5.5	6.95	L[001]	3.63	5.5	⊥	2.39	14.6	23.9	24
BGO	0.45...7.5	9.22	L[110]	3.42	1.6	Arb.	2.55	3.8	6.7	6.7
TeO_2	0.35...5.0	6.0	S[110]	0.62	17.9	Cir.	2.26	13.1	795	127
GaP	0.6...10.0	4.13	L[110]	6.32	8.0	‖	3.31	75.3	29.5	71
			S[110]	4.13	2.0	⊥	3.31		16.6	26
Hg_2Cl_2	0.30...28.0	7.18	S[110]	0.347	8.0	‖	2.27	4.3	703	73
GaAs	1.0...11.0	5.34	L[110]	5.15	15.5	‖	3.37	118	69	137
GeAsSe-glass	1.0...14.0	4.4	L	2.52	1.7	⊥	2.7	54.4	164	129
Ge	2.0...22.0	5.33	L[111]	5.5	16.5	‖	4.0	1117	482	1214
Tl_3AsS_4	0.6...12.0	6.2	L[001]	2.15	5.0	‖	2.83	1.52	523	416
Tl_3AsSe_3	1.26...13.0	7.83	L[100]	2.05	14.0	‖	3.34	607	2259	1772

L: longitudinal mode; S: shear mode.

7.1.5.3 Acousto-optic intensity modulator

In an analog acousto-optic modulator the acoustic wave is Amplitude-Modulated (AM) and the incident laser beam is focused onto the sound grating as shown in Fig. 7.1.9. As already described for bandwidth considerations the ratio of divergences of light beam and acoustic beam should be near 1. The three acoustic waves, namely carrier, the upper, and the lower sidebands will generate three correspondingly diffracted light waves traveling in separate directions. The modulated light intensity is determined by overlapping collinear heterodyning of the diffracted optical carrier beam and the two sidebands. The focused-beam-type modulator has certain disadvantages. The diffraction spread associated with the narrow optical beam tends to lower the diffraction efficiency. More importantly, the focusing of the incident beam results in a high peak intensity that can cause damage for even relatively low laser power levels. Then it is necessary to open up the optical aperture. Due to the basic issues of acoustic transient time, the temporal bandwidth of the modulator will be severely degraded.

A variety of acousto-optic modulators are commercially available suited for external or intracavity applications. Compared to the competing electro-optic modulators, the acousto-optic modulators have some advantages that include low driving power, high extinction ratio, and insensitivity to temperature change. When bandwidths below the GHz range are required, acousto-optic modulators are mostly preferred to their electro-optic counterparts. Low-cost types, usually made of special glasses, are useful for bandwidth up to about 10 MHz. The use of superior materials such as $PbMoO_4$ and TeO_2 has raised the modulation bandwidth up to about 50 to 100 MHz. And a GaP modulator can operate down to about 2 ns rise time, which corresponds to a maximum modulation bandwidth of about 500 MHz. Table 7.1.6 lists a few selected acousto-optic modulators with some of their typical parameters.

Table 7.1.6. Typical performances of a few selected acousto-optic modulators [95Cha].

Material	Wavelength λ [μm]	Center frequency f_0 [MHz]	RF bandwidth Δf [MHz]	Rise time t_r [ns]	Diffraction efficiency η [%]
$PbMoO_4$	0.633	80	40	25	80
TeO_2	0.633	110	50	20	75
TeO_2	0.633	200	100	7	65
GaP	0.83	500	250	4	50
GaP	0.83	1000	500	2	30

GeAsSe glass is particularly suited to wideband applications at 1.06 μm wavelength due to its exceptionally low acoustic loss (1.7 $dB/(\mu s \cdot GHz^2)$). At 10.6 μm, the most popular material is single-crystal Ge. A Ge modulator shows a typical rise time of 30 ns and an efficiency of 5%/Watt. Acousto-optic materials with high optical quality, such as fused silica, are exclusively used inside a laser cavity. These applications include Q-switching, mode locking, and cavity dumping.

7.1.5.4 Acousto-optic deflector

Basically, acousto-optic deflectors operate in the same way as acousto-optic Bragg modulators; the main difference is that the frequency rather than the amplitude of the sound wave is modulated – Frequency-Modulated (FM) wave. Figure 7.1.10 shows the operation principle of a Bragg deflector.

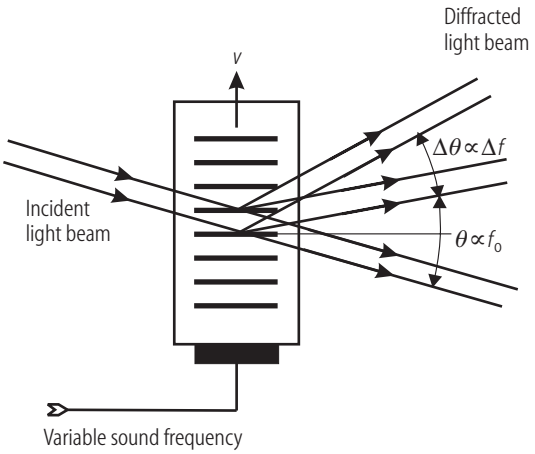

Fig. 7.1.10. Bragg diffraction acousto-optic deflector (Bragg cell).

Basic equation for this application is

$$\Delta\theta = \frac{\Delta f \cdot \lambda}{nv \cdot \cos\theta_{\mathrm{B}}} \ . \tag{7.1.44}$$

In a deflector, the most important performance parameters are resolution and speed. Therefore, the divergence of the optical beam should be small, see Fig. 7.1.10. Resolution, or the maximum number of resolvable spots, is defined as the ratio of the range of deflection angle divided by the angular spread of the diffracted beam. Taking the angular beam divergence in case of a Gaussian beam as

$$\delta\theta_0 = \frac{2\lambda}{\pi n\bar{d}}$$

it results in

$$N = \frac{\Delta\theta}{\delta\theta_0} = \frac{\pi\bar{d}}{2v \cdot \cos\theta_{\mathrm{B}}} \cdot \Delta f \approx \tau \cdot \Delta f \ , \tag{7.1.45}$$

where $\tau = \bar{d}/v$ is the acoustic transit time across the optical aperture. A common figure of merit is the ratio of the total number of resolvable spots to the access time, determined by the feasible bandwidth according to

$$\frac{N}{\tau} = \Delta f \ . \tag{7.1.46}$$

Thus, a high speed–capacity product is only achievable when the bandwidth is large, which requires, as in the case of a modulator, a high modulation frequency f of the device. Basically, there is a trade-off between the speed and the resolution of AO deflectors. The maximum resolution is limited to a few thousands. Table 7.1.7 shows examples of some acousto-optic deflectors (Bragg cells).

Besides bandwidth, the acoustic attenuation across the aperture is a basic parameter, which in most solids is proportional to the square of the acoustic frequency, i.e. f^2. For an allowable average attenuation across the band, $\bar{\alpha}$ [dB], the maximum deflector resolution can be estimated as

$$N_{\max} = \frac{\bar{\alpha}}{\alpha_{\mathrm{a}} \cdot f_0} \ , \tag{7.1.47}$$

where α_{a} [dB/(μs · GHz^2)] is the acoustic attenuation coefficient and f_0 is the center frequency.

Table 7.1.7. Performance of acousto-optic Bragg cells at $\lambda = 830$ nm [95Cha].

Material	Center frequency f_0 [MHz]	Bandwidth Δf [MHz]	Access time τ [μs]	Resolution $N = \tau\Delta f$	Efficiency η [% / W]
TeO_2 (S)	90	50	40	2000	110
TeO_2 (S)	160	100	10	1000	95
GaP (S)	1000	500	2.0	1000	30
GaP (S)	2000	1000	1.0	1000	12
$LiNbO_3$ (S)	2500	1000	1.0	1000	10
GaP (L)	2500	1000	0.25	250	44
GaP (L)	3000	2000	0.15	300	10
GaP (S)	3000	2000	0.25	500	8
$LiNbO_3$ (S)	3000	2000	0.30	600	6

L: longitudinal mode; S: shear mode.

7.1.6 Glossary

$\boldsymbol{D}$	displacement vector
$\boldsymbol{E}$	electric field vector
c	velocity of light in vacuum
d	width of the electro-optic crystal
$\bar{d}$	optical beam width
f	acoustic frequency
$(\Delta f)_\mathrm{m}$	modulation bandwidth
H	acoustic beam height
I	intensity
$\boldsymbol{k}$	optic wave vector
k	optic wave number
$\boldsymbol{K}$	acoustic wave vector
K	acoustic wave number
L	length of the electro-optic crystal, acoustic beam width
M	figure of merit
N	number of resolvable spots
n	optical refractive index
n_x, n_y, n_z	principal indices of refraction
$\Delta\left(\frac{1}{n^2}\right)$	change in an impermeability tensor element
K	Kerr constant
P_a	acoustic power
p	strain-optic coefficient
r	linear electro-optic coefficient
s	quadratic electro-optic coefficient
S	strain
v	sound velocity
V	applied voltage
V_π	half-wave voltage
(x, y, z)	principal dielectric coordinate system
(x', y', z')	perturbed principal dielectric coordinate system

α_a	acoustic attenuation
δ	phase modulation index
ϵ	dielectric constant
η	diffraction efficiency
κ	coupling constant
λ	vacuum wavelength of light
ϕ	deflection angle
ρ	mass density
σ	modulation index reduction factor
τ	transit time
ν_m	modulation frequency
ω	light radian frequency
ω_m	modulation radian frequency
Φ	phase of the optical field
$\Delta\Phi$	phase shift of light
Γ	phase retardation
Γ_m	amplitude modulation index
Λ	acoustic wavelength
θ_B	Bragg angle
$\delta\theta_o$, $\delta\theta_a$	beam divergence: optical, acoustic
Ω	acoustic radian frequency

References for 7.1

61Nam Namba, C.S.: J. Opt. Soc. Am. **51** (1961) 76.
61Woo Woodruff, T.O., Ehrenreich, H.: Phys. Rev. **123** (1961) 1553.

66Gor Gordon, E.I.: Appl. Opt. **5** (1966) 1629.

67Dix Dixon, R.W.: J. Appl. Phys. **38** (1967) 3634.
67Kam Kaminow, I.P., Sharpless, W.M.: Appl. Opt. **6** (1967) 351.
67Kle Klein, W.R., Cook, B.D.: IEEE Sonics Ultrason. **14** (1967) 123.
67Nye Nye, J.F.: Physical Properties of Crystals, Oxford: Clarendon Press, 1967.

72Den Denton, R.T.: Laser handbook, Arecchi, F.T., Schulz-DuBois, E.O. (eds.), Amsterdam: North Holland Publ. Co., 1972, p. 703–724.
72Kor Korpel, A.: Acousto-Optics, Applied Solid State Science, Vol. 3, Wolfe, R. (ed.), New York: Academic Press, 1972.
72Pin Pinnow, D.A.: Laser handbook, Arecchi, F.T., Schulz-DuBois, E.O. (eds.), Amsterdam: North Holland Publ. Co., 1972, p. 995–1008.
72Wem Wemple, S.H.: Laser handbook, Arecchi, F.T., Schulz-DuBois, E.O. (eds.), Amsterdam: North Holland Publ. Co., 1972, p. 975–994.

75Yar Yariv, A.: Quantum Electronics, New York: J. Wiley & Sons, 1975.

79Coo Cook, W.R., Jaffe, H.: Landolt Börnstein, Vol. III/11, Hellwege, K.-H. (ed.), Heidelberg: Springer-Verlag, 1979, p. 287.
79Hel Hellwege, K.-H.: Landolt Börnstein, Vol. III/11, Heidelberg: Springer-Verlag, 1979.

84Yar Yariv, A., Yeh, P.: Optical waves in crystals, New York: J. Wiley & Sons, 1984.

86Got Gottlieb, M.: Handbook of laser science and technology, Vol. IV, part 2, Boca Raton, Fl.: CRC Press, 1986, p. 319–341.
86Kam Kaminow, I.P.: Handbook of laser science and technology, Vol. IV, part 2, Boca Raton, Fl.: CRC Press, 1986, p. 253–278.

89Gha Ghatak, A., Thyagarajan, K.: Optical electronics, New York: Cambridge Univ. Press, 1989.

90Alf Alferness, R.C.: Guided wave optoelectronics, Chap. 4, Tamir, T. (ed.), New York: Springer-Verlag, 1990.

92Dol Dolfi, D.W., Ranganath, T.R.: Electron. Lett. **28** (1992) 1197.

95Cha Chang, I.C.: Handbook of optics II, New York: McGraw-Hill, Inc., 1995, p. 12.1–12.54.
95Mal Maldonado, T.A.: Handbook of optics II, New York: McGraw-Hill, Inc., 1995, p. 13.1–13.35.

97Lee Lee, N.L.: Handbook of photonics, Gupta, M.C. (ed.), New York: CRC Press, 1997, p. 393–434.

02Tak Takeuchi, H., Saitho, T., Ito, H.: Technical Digest OFC2002, WV1.